

Magnetic edge states in MoS₂ characterized using density-functional theoryAleksandra Vojvodic,^{1,2,*} Berit Hinnemann,³ and Jens K. Nørskov²¹*Department of Applied Physics, Chalmers University of Technology, SE-412 96 Göteborg, Sweden*²*Center for Atomic-scale Materials Design, Department of Physics, Technical University of Denmark, DK-2800 Kgs. Lyngby, Denmark*³*Haldor Topsøe A/S, Nymøllevej 55, DK-2800 Kgs. Lyngby, Denmark*

(Received 23 April 2009; revised manuscript received 10 July 2009; published 18 September 2009)

It is known that the edges of a two-dimensional slab of insulating MoS₂ exhibit one-dimensional metallic edge states, the so-called “brim states.” Here, we find from density-functional theory calculations that several edge structures, which are relevant for the hydrodesulfurization process, are magnetic. The magnetism is an edge phenomenon associated with certain metallic edge states. Interestingly, we find that among the two low-index edges, only the S edge displays magnetism under hydrodesulfurization conditions. In addition, the implications of this on the catalytic activity are investigated. Despite large changes in the magnetic moments, a small influence on the adsorption energies is observed. This has implications on the suitability of magnetic measurements for monitoring the catalytic properties.

DOI: [10.1103/PhysRevB.80.125416](https://doi.org/10.1103/PhysRevB.80.125416)

PACS number(s): 73.20.At, 75.75.+a, 73.22.-f

I. INTRODUCTION

Layered compounds such as graphite^{1–3} and MoS₂ (Refs. 4–7) are known to exhibit metallic edge states. For graphite, some of these edge states have been found to be magnetic.^{1,8–12} In the present paper, we discuss the possibility of magnetic edge states for MoS₂.

MoS₂ has a structure which is equivalent to graphite with hexagonal S-Mo-S sheets held together by van der Waals forces. Therefore, some of the properties of MoS₂ are similar to graphite, such as its semimetallic nature and its use as a lubricant.^{13,14} Another important application of MoS₂ is its use as a hydrodesulfurization (HDS) catalyst, which removes sulfur compounds from crude oil.¹⁵ Typically, Co- or Ni-promoted catalysts are used for HDS, but unpromoted MoS₂ has also some catalytic activity. Previous experimental and theoretical studies^{15–22} have shown that only the edges are catalytically active and that the metallic edge states, also termed “brim states,” play an important role for the activity. Thus, the presence of metallic edge states is also important from a catalysis point of view.

Even though bulk MoS₂ is known to be nonmagnetic low-dimensional structures of MoS₂ that exhibit magnetism have been synthesized. It is possible to grow MoS₂ nanotubes²³ and in a recent study, Li-doped MoS₂ nanotubes with a susceptibility 100 times larger than the one of pure Li metal were fabricated.²⁴ The susceptibility was attributed to the presence of magnetic states in the MoS₂ nanotubes themselves rather than to the presence of Li. First-principle simulations of MoS₂ nanotube bundle systems have been performed in Ref. 25. A theoretical study on small three-dimensional (3D) (MoS₂)_n clusters showed that some of them are magnetic.²⁶ Magnetic properties were also observed for supported MoS₂ particles in Ref. 27. Based on the hysteresis curves for particles with different sizes, Zhang *et al.* concluded that the magnetic states must be located at the particle edges, since smaller particles give rise to larger magnetization. Zhang *et al.*²⁷ also performed spin-polarized density-functional theory (DFT) calculations on triangular-shaped clusters showing that magnetic states are present for

clusters terminated by 0% S-covered Mo edge and 100% S-covered S edge. The magnetism was related to the presence of edge spins on the prismatic edges of the triangular nanosheets.

In the present paper, we investigate the magnetic states in MoS₂ in the context of HDS catalysts. We place particular emphasis on the question, whether magnetic edge states are present in MoS₂ under actual HDS conditions, i.e., in the presence of H₂ and H₂S at certain temperatures and pressures. While it seems plausible that the Mo edge with uncoordinated Mo atoms exhibits a magnetic moment, it is not clear if the same edge under HDS conditions, at which it is terminated with sulfur dimers or monomers, would be magnetic. In addition, we want to single out the edge effects and therefore consider a periodic stripe model as in Ref. 6 to eliminate contributions from the corners. In the following, the characteristics of interest are (i) if the magnetism is a surface phenomena, (ii) at what edge termination(s) the magnetic states are present, (iii) with which chemical species (Mo, S, or both) they are associated, (iv) how deep in the structure the magnetism extends, and (v) what the strength of the magnetism is. In addition, we investigate the influence of the magnetism on the catalytic activity and what happens under scanning tunneling microscope (STM) and realistic HDS conditions.

First we present the model and the computational method used in this paper. This is followed by a detailed study of the formation of S vacancies and H adsorption, two of the important steps in the HDS reaction catalyzed by MoS₂. Finally, implications of our findings are discussed and compared with existing experiments.

II. MODEL

Bulk MoS₂ is a layered material consisting of S-Mo-S layers. In each layer the Mo atoms are positioned in a hexagonal lattice and are coordinated to six S atoms in a trigonal prismatic coordination. The two possible low-index edge terminations of a single layer of MoS₂ are the (10 $\bar{1}$ 0) edge (Mo

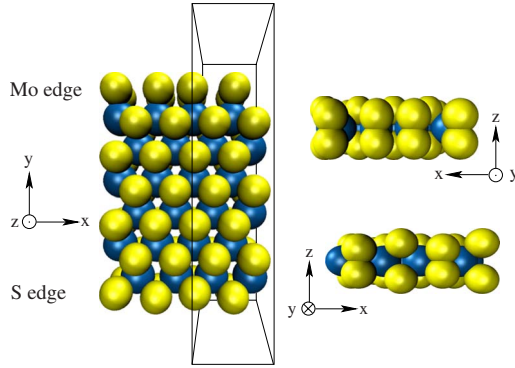


FIG. 1. (Color online) Illustration of the stripe model utilized in our study of the single-layered MoS₂ stripe. Shown is the MoS₂ structure with 100% sulfur coverage on both the Mo and the S edge, which are indicated in the left figure. To the right a side view of the two edges is shown. The slab consists of 2(6) rows of Mo atoms in the $x(y)$ direction, also denoted as (2,6). The yellow (light) and blue (gray) balls represent the S and Mo atoms, respectively.

edge) and the $(\bar{1}010)$ edge (S edge). The MoS₂ nanoparticles are treated within a stripe model (Fig 1).⁶ In this model, periodic boundary conditions are used on a slab consisting of a single MoS₂ layer with (2,6) rows, which corresponds to two (six) rows in the $x(y)$ direction. The stripes are separated with 14.8 Å (10.4 Å) vacuum in the $z(y)$ direction. In this kind of supercell, both the Mo edge and the S edge are present simultaneously. The supercell is constructed so that it can take into account the reconstruction that are two periods wide^{6,28} and to prevent interaction of the two edges. Convergence test with respect to the stripe width have been conducted in Refs. 4 and 6 and demonstrated that energies as well as STM simulations of the edges are well converged for the six-units wide stripe. Furthermore, we demonstrate in Sec. III B, that in the middle of the slab the local density of states (LDOS) as well as the Bader charges are identical to the ones in bulk MoS₂. Also these findings indicate that in the six-units wide stripe the edges are decoupled. This kind of model has earlier proved to be applicable for studies of unsupported type II MoS₂, which are found in well-established industrial HDS catalysts.²⁹

In the stripe model, an atom is either an edge atom, if it belongs to the outermost S and/or Mo atomic layer, or a bulk atom. Hence any possible origin of magnetism from the edge states should be captured by this model.

All calculations have been performed with the DFT code DACAPO.^{30,31} We use 30 Ry plane-wave cutoff, 45 Ry density cutoff, a $6 \times 1 \times 1$ k -point sampling (equivalent to the one used in Ref. 6), and the revised Perdew-Burke-Ernzerhoff (RPBE) exchange-correlation functional.³² The Fermi temperature is set to 0.1 eV and all energies are extrapolated to zero electronic temperatures. All structures are allowed to relax until all forces are less than 0.02 eV/Å (corresponding to total energy changes less than 10^{-8} eV). The dipole correction implemented in DACAPO has been used.³³

The calculated hexagonal lattice constant of MoS₂ is 3.235 Å, which agrees well with the experimental value of 3.16 Å.³⁴ The RPBE functional overestimates the layer

separation between two S-Mo-S layers, since generalized gradient approximation functionals do not capture van der Waals forces.³⁵ However, we only consider a single layer of S-Mo-S in this study, and therefore van der Waals forces are not of importance.

First, non-spin-polarized then spin-polarized calculations are performed, in each step allowing all the atoms to relax. The spin-polarized structures are initially given either ferromagnetic or antiferromagnetic symmetry. Several initial ferromagnetic structures were investigated with the initial magnetic moments of the S atoms always set to zero and the ones of the Mo atoms either all set to $2\mu_B$ or $1\mu_B$. For the antiferromagnetic structures, the magnetic moments were initialized to zero for S and either $\pm 2\mu_B$ or $\pm 1\mu_B$ in an alternating fashion. We find that the resulting magnetic moments do not depend on the magnitude of the initial magnetic moment.

To be able to systematically monitor the changes in the magnetic properties, we investigate MoS₂ stripes with different S coverages. The considered structures are those where the Mo and the S edges have a 25%, 50%, 75%, or 100% S coverage. An S coverage of 100% corresponds to two S edge atoms per one Mo edge atom. In the calculation the variations in the S coverage are done on only one side of the slab at the time, while the S coverage on the other edge is fix at 100%.

The stripes are terminated differently depending on the environmental conditions. Here we focus on the STM conditions, where $T=300$ K, $p_{H_2}=2 \cdot 10^{-16}$ bars, and $p_{H_2S}=1 \cdot 10^{-13}$ bars, and HDS conditions, where $T=650$ K, $p_{H_2}=10$ bars, and $p_{H_2S}=0.1$ bars.⁶

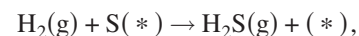
To gain a deeper understanding of the magnetism, we utilize electronic structure analysis tools, such as electron density differences, Bader charge analysis,^{36,37} and atom projected density of states to elucidate the strength and spatial distribution of the magnetic states.

III. S VACANCY FORMATION

In this section, we present the results and analysis of the influence of the magnetic coupling on the S vacancy formation. First, the geometry, energetics, and total magnetic moments are presented in Sec. III A. As energy differences as such do not provide any information of the exact location, strength, or origin of the magnetic states, the focus in Sec. III B is on the analysis of the electronic structure, which can give such information. Sec. III C deals with the intricate interplay between the edge configuration and the appearance of magnetism.

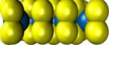
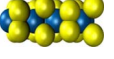
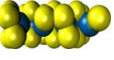
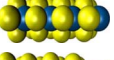
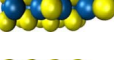
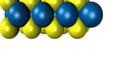
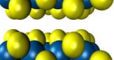
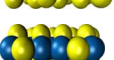
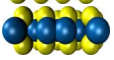
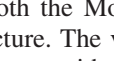
A. Energetics and magnetic moments

At the edges of the MoS₂ stripe, sites with a coordination number of Mo lower than six can be created by removal of sulfur. These coordinatively unsaturated sites are defined as S vacancies and can be created by the following reaction between H₂S, H₂, and the MoS₂ surface



with (*) denoting an S vacancy. In the following, we take the fully sulfurized stripe, the structure where the S coverage

TABLE I. (Color online) Given are the relaxed MoS₂ structures, the nomenclature (Nom.), the non-spin-polarized S vacancy formation energies (E_S) the changes in energy per Mo atom row for the ferromagnetic ($\Delta E_S^{\text{ferro}}$) and the antiferromagnetic (ΔE_S^{anti}) states compared with E_S . All energies are in eV. The last column (Pos.) specifies at which edge(s) [either S, and/or Mo, or none] the magnetism is located as determined by a Bader analysis. The Mo100S100 structure is used as reference. As the S coverage on one edge is varied, the S coverage on the other edge is kept at 100%.

Structure	Nom.	E_S	$\Delta E_S^{\text{ferro}}$	ΔE_S^{anti}	Pos.
	Mo100S100	Ref.	-0.023	0.023	S
					
Mo edge					
					
					
	Mo75	0.221	-0.023	0.000	S
	Mo50	-0.421	-0.024	0.000	S
	Mo25	0.204	-0.029	0.000	S
	Mo0	2.919	-0.086	-0.044	Mo/S
S edge					
	S75	0.113	0.000	0.000	
	S50	0.551	-0.001	0.000	
	S25	2.474	0.000	0.000	
	S0	5.259	-0.015	0.000	S

is 100% on both the Mo and the S edge (Mo100S100), as reference structure. The vacancy formation energy (E_S) of a particular structure with n sulfur atoms removed can be obtained as

$$E_S = E[\text{MoS}_2 + n(*)] + nE(\text{H}_2\text{S}) - E[\text{MoS}_2 + n\text{S}] - nE(\text{H}_2), \quad (1)$$

where $E[\text{MoS}_2 + n\text{S}]$ is the non-spin-polarized (spin-polarized) energy of the reference structure, $E[\text{MoS}_2 + n(*)]$ is the non-spin-polarized (spin-polarized) energy of a certain stripe with n S vacancies, and $E(\text{H}_2\text{S})$ and $E(\text{H}_2)$ are the energies of spin-polarized isolated molecules, respectively.

The geometries of the non-spin-polarized and the spin-polarized structures are very similar. The largest difference was found for the Mo0 stripe, where the outermost Mo atoms moved a distance of 0.079 Å compared with its position in the non-spin-polarized structure. For the other structures, the difference was smaller than 0.030 Å.

Table I summarizes the non-spin-polarized E_S values obtained from our calculations. The relative energetics of the investigated non-spin-polarized stripes is in agreement with the results in Ref. 6 (performed with the PW91 xc functional) and Ref. 28. Studies have shown that under sulfiding

and STM conditions,⁶ the Mo edge is terminated by sulfur dimers, whereas under HDS conditions¹⁹ the Mo edge is terminated by sulfur monomers, that is, Mo50 (with adsorbed hydrogen, to be discussed later). The S edge is under most relevant conditions terminated by sulfur dimers, that is, S100 (possibly with adsorbed hydrogen, to be discussed later).

When it comes to spin-polarized calculations, we find that several structures prefer to be in a magnetic state (see Table I) even though the energy gain compared to the non-spin-polarized structures is small and comparable to thermal energies. This implies that the magnetic and nonmagnetic states may coexist or compete with each other. Independently of the initial magnetic moment (see Sec. II) of a given configuration, the same final total magnetic moment was obtained.

Of the structures initialized with a ferromagnetic symmetry, we find that after relaxation the reference structure Mo100S100, all the Mo-edge structures, that is, Mo0, Mo25, Mo50, and Mo75, and the S0 structure are ferromagnetic. It should be stressed that a ferromagnetic structure is here defined as a structure where all the Mo atoms have the spins aligned in the same direction.

In contrast, most structures initialized as antiferromagnetic loose their magnetic moment during the relaxation and converge to their nonmagnetic equivalent. Only the Mo0 structure has a stable antiferromagnetic state, however, the

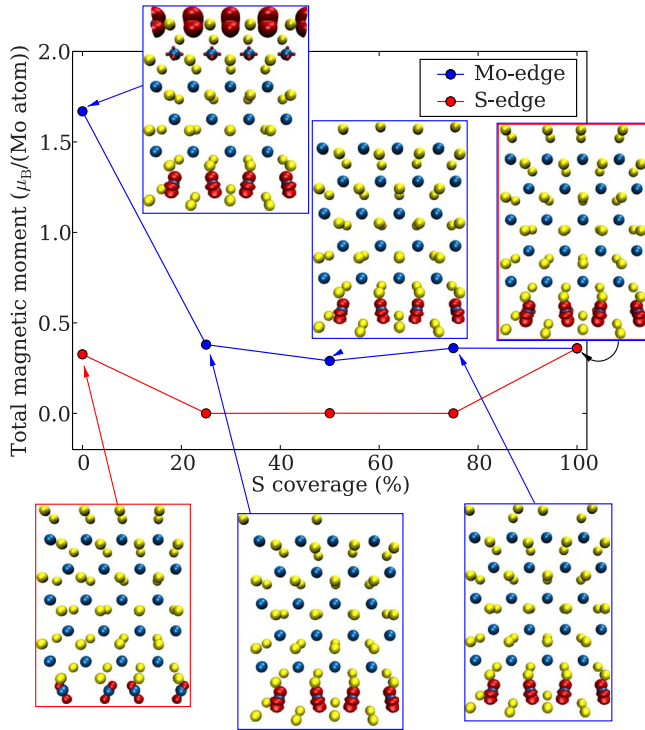


FIG. 2. (Color online) Total magnetic moments averaged per edge Mo atom of the considered Mo- and S-edge ferromagnetic structures as a function of the S coverage in blue and red, respectively. Also, presented are the structures together with the 3D spatial localizations of the magnetization ($n_{\uparrow} - n_{\downarrow}$) in red. The structures with no net magnetic moment are not provided since they are redundant. The color coding of the atoms is the same as in Fig. 1.

ferromagnetic state is lower in energy. Therefore, we only consider ferromagnetic structures in the rest of the study. This restriction is supported by the fact that under STM and HDS conditions, neither a completely S stripped Mo edge nor a completely S stripped S edge is present (see the phase diagrams in Ref. 6).

In Fig. 2, the evolution of the total magnetic moments as a function of the S coverage is presented together with the difference in spin-up and spin-down electron densities (n_{\uparrow} and n_{\downarrow} , respectively), which gives a representation of the magnetization in real space. Based on the geometry of the Mo atoms at the S edge and the form of the charge-density difference (Figs. 2 and 3), we conclude that they contribute equally to the magnetization.

For all the magnetic structures, we find that there is always a contribution from the edge Mo atoms at the S edge (see Fig. 2). The Mo edge is only magnetic in the Mo0 structure. Inside the stripe, no magnetization is observed, which agrees with the well-known fact that bulk MoS_2 is nonmagnetic.

Figure 3 provides a detailed illustration of the spatial localization of the magnetism for the Mo100S100 structure. The magnetic states are located exclusively on the S edge with the main contribution from the Mo atoms. They do not extend into the bulk but protrude slightly towards the vacuum and the undimerized S edge atoms. The symmetry of these magnetic states is of a clear d character. There is also a

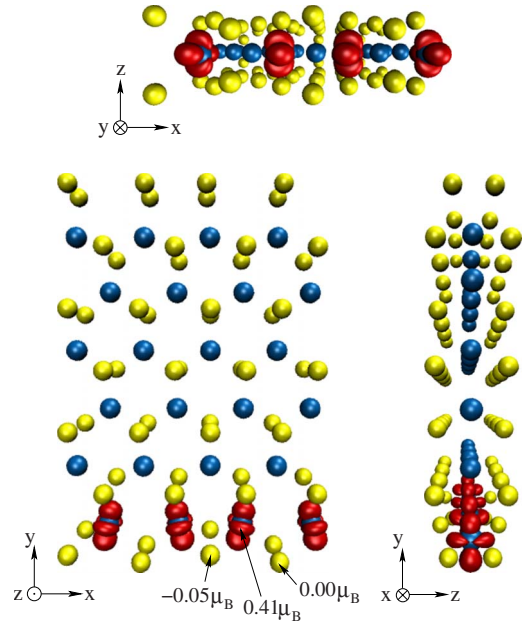


FIG. 3. (Color online) Visualized in red is the 3D real space localization of the magnetization (for a representative isosurface with the value $0.05/\text{\AA}^3$) and the local magnetic moments obtained by a Bader analysis (see text for more details). The magnetic states have a pure d character associated with the Mo edge atoms on the S edge. In addition, an order of magnitude smaller magnetization is found on the undimerized S edge atoms on the S edge (not visible for the chosen isosurface). The color coding of the atoms is the same as in Fig. 1.

small contribution to the magnetization from the S atoms which appears at much lower isosurface values (for more details see Sec. III B).

In conclusion, the magnetization of the MoS_2 stripes is purely an edge phenomenon. We have found a ferromagnetic configuration, the S edge with 100% sulfur coverage, which is relevant for both STM and HDS conditions. The magnetism in this structure is mainly localized on the edge Mo atoms just as the metallic edge states identified in Ref. 4. For all Mo edge structures present under realistic HDS conditions, no magnetism is observed.

B. Electronic structure analysis of the local magnetic moments

To better understand the origin of the magnetism, we calculate the local magnetic moments of each atom in the stripe. This involves partitioning of the charge density around the different atoms, however there is not a single and well-defined way to do this. To alleviate the influence of the partition choice several different methods are used.

In the first method, the local magnetic moments are obtained by two different Bader approaches either (i) by performing a Bader analysis on $n_{\uparrow} - n_{\downarrow}$ or (ii) by calculating the Bader charges for n_{\uparrow} and n_{\downarrow} separately and then taking the difference between the two.^{36,37} The two approaches give the same overall picture but differ slightly in the absolute numbers (see Table II), due to the finite density grid including noise. Convergence has been tested with respect to the integration grids and other parameters.

TABLE II. Local magnetic moments for the Mo atoms on the S edge of the Mo100S100 structure calculated by four different methods (see text for details).

Method	Mo	S mono	S in dimer	M_{tot}
Bader($n_{\uparrow} - n_{\downarrow}$)	0.41	-0.05	0.00	0.72
Bader(n_{\uparrow}) - Bader(n_{\downarrow})	0.50	-0.08	0.00	0.72
LDOS(short)	0.12	-0.01	0.00	0.21
LDOS(infinite)	0.35	-0.05	0.00	0.60

The second method is based on the LDOS's. By individually integrating the spin-up and spin-down LDOS's up to the Fermi level and taking the difference between the two gives the local magnetic moment. To investigate the methods sensitive on the projection radius, we have performed calculations with a cut-off radius of 1 Å (short) and with no cut-off radius (infinite) (see Table II). The short radius gives lower magnetic moments, which is because it cannot take the covalent bonding with electron density between the Mo and S atoms into account. Therefore, the infinite radius projection is used, which is able to take into account the covalent bonding, and gives a consistent picture with the Bader approach (i). In the following we therefore choose to present the local magnetic moments from only one of them namely the Bader analysis of approach (i).

A Bader analysis of the spin-polarized Mo100S100 stripe shows that (i) the localization of the magnetic states is attributed to the S edge (see Fig. 3), (ii) that there is no magnetism in the interior of the stripe, and (iii) that each edge Mo atom contributes equally to the magnetization with $0.41\mu_B$, in agreement with results based on the real-space magnetization plots in Sec. III A. In addition, we find that the undimerized S atoms have, in contrast to the dimerized ones, a magnetic moment of $-0.05\mu_B$ (see Fig. 3). In the interior of the stripe a charge transfer from Mo to S takes place. These Mo atoms donate 1.86 electrons and each S atom gains 0.93 electrons yielding an ionic contribution to the MoS₂ bond, as in the bulk MoS₂. Hence, there is no interaction between the Mo and the S edge, which confirms that the (2,6) slab is a good representation of the stripes.

The slightly preferred stability in the ferromagnetic structure can to some extent be rationalized with help of the LDOS's. Figure 4 shows the non-spin-polarized LDOS's for relevant atoms in the Mo100S100 stripe. In the interior of the stripe, the LDOS resembles the bulk DOS with a band gap of 1.46 eV, experimentally the gap is 1.78 eV.³⁴ This discrepancy is the well-known underestimation of band gaps encountered in DFT.³⁸ Both at the Mo and the S edge there is metallic surface state in agreement with previous findings.⁴ The surface state at the S edge is more pronounced than the one localized at the Mo edge. It should be emphasized that the metallic edge states are not a consequence of dangling bonds, since the edge Mo atoms are fully coordinated, but due to subtle changes in the electronic structure at the edge.

In general, the presence of surface states in the vicinity or at the Fermi level makes a system less stable. By introducing the magnetic interaction, the system may overcome this instability by rearranging its states in the spirit of a spin-Peierls

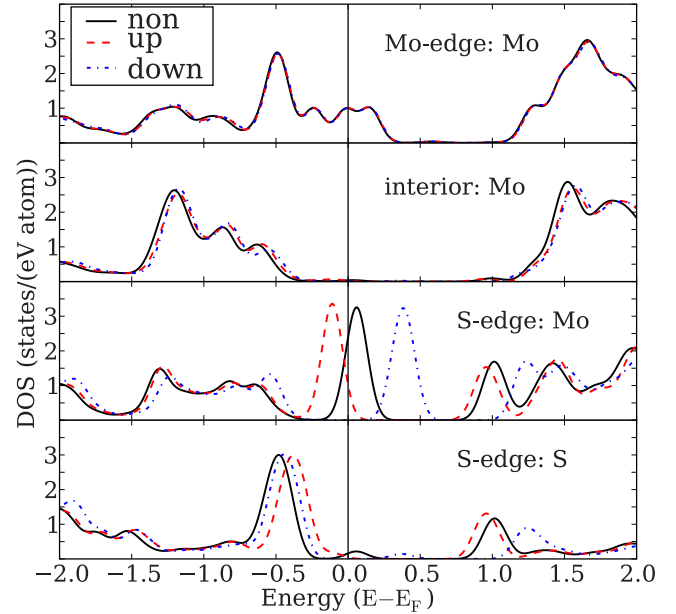


FIG. 4. (Color online) Calculated non-spin-polarized (black solid line) and spin-polarized (red dashed and blue dashed-dotted lines) atom projected DOS for the Mo100S100 structure for (from above) a Mo atom at the Mo edge, in the interior of the stripe, and at the S edge, and an undimerized S atom at the S edge.

instability.³⁹ Figure 4 shows the spin-polarized LDOS's for the Mo100S100 structure. No splitting of the LDOS is found in the interior of the stripe or at the Mo edge and hence no magnetism is localized here. However, at the S edge there is a splitting of the Mo *d* edge states in the vicinity of the Fermi level. In addition, a hybridization between the Mo *d* and the undimerized S *p* states results in a splitting of the S states at the S edge, associated with the small local magnetic moment found by the Bader analysis. The symmetry breaking upon introduction of spin-spin interaction has been studied among others by Stoner⁴⁰ and Gunnarsson.⁴¹

Upon change of the S coverage at the edge, there is a change in the LDOS and therefore the magnetic situation may change. A splitting of the LDOS is found for the Mo0 and the S0 structure (Fig. 5). For these structures, the edges are terminated by Mo atoms, which have a lower coordination number than Mo in the bulk, resulting in a build-up of

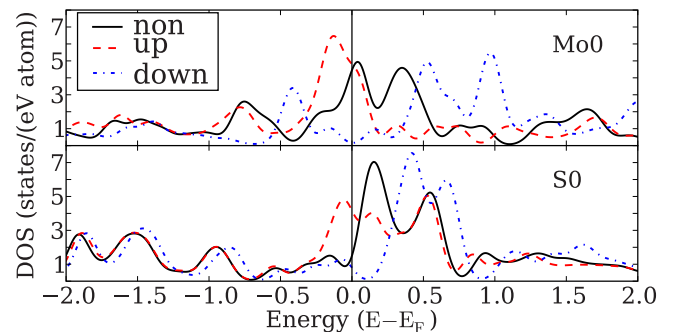
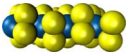
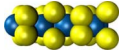
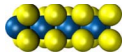


FIG. 5. (Color online) Calculated non-spin-polarized and spin-polarized LDOS's for a Mo atom at the Mo edge for the Mo0 structure and a Mo atom at the S edge for the S0 structure.

TABLE III. (Color online) Given are the non-spin-polarized energies relative to the reference structure, ΔE_S , and the spin-polarized energies relative to the corresponding non-spin-polarized structures, ΔE_{ferro} , for the S100dd, S100du, and S100uu structure. Energies are in eV/(unit cell). The Mo edge is kept fix in the S dimer configuration. Also given are the total magnetizations, M_{tot} , (in μ_B /unit cell), the local magnetic moments of the Mo atom, M_{Mo} , and of one of the S atoms in each S pair, M_{S_i} with $i=1,2$ (in μ_B /atom), obtained by a Bader analysis. For the S100du structure M_{S_1} is the local magnetic moment of the undimerized S atom. The absolute sulfur formation energy of the reference structure can be found in Table I.

Structure	ΔE_S	ΔE^{ferro}	M_{tot}	M_{Mo}	M_{S_1}	M_{S_2}
	0.031	-0.005	0.000	0.00	0.00	0.00
	Ref.	-0.046	0.719	0.41	-0.05	0.00
	0.622	-0.111	1.265	0.13	-0.35	-0.35

states at the Fermi level. These configurations are not relevant under HDS conditions⁶ and therefore we do not discuss them further. The Mo and S edge structures with other S coverages have significantly lower number of states at the Fermi level and the spin-up and spin-down states remain degenerate.

In conclusion, the calculated local magnetic moments and the LDOS results complement the results from the real space magnetization plots. They also provide us with the physics behind the appearance of magnetism.

C. Interplay between dimerization and magnetism

Based on our finding that magnetism is present at the 100% S-covered S edge, which is highly relevant both under STM and HDS conditions, we investigate the influence of different S pair configurations on the magnetism.

In previous studies,^{6,29} it was shown that there are several stable structures for the S edge terminated by 100% sulfur. Here we consider a fully sulfurized MoS₂ stripe with the S pairs at the S edge in one of the three configurations (depicted in Table III): (a) both dimerized (S100dd), (b) one dimerized and one undimerized, that is, the S atoms are monomers (S100uu, previously denoted as Mo100S100), and (c) both undimerized (S100uu). The most stable structure is the S100du structure, closely followed by the S100dd structure, which is only 0.03 eV higher in energy. In contrast, the S100uu structure, with no dimers, is 0.6 eV higher in energy than the S100du structure. Thus, energy is gained by dimerization, as we also know from the 100% S-covered Mo edge where all S pairs are dimerized and each of them coordinated to one edge Mo atom. At the S edge, however, each S pair is coordinated to two edge Mo atoms, and therefore the dimerization happens at the expense of Mo-S interaction. Thus, it is most favorable to only dimerize every second S pair and still preserve good Mo-S interaction by every other undimerized pair.

This competition between the S-S and the Mo-S interactions at the edges should also influence the tendency of each of these three structures to magnetize. From our previous results, the hypothesis would be that the stronger the Mo-S

interaction, the higher the tendency of the structure to magnetize.

We find that the magnetization of the three configurations can be ordered as: S100dd < S100du < S100uu. The magnetic moment of the S100uu structure is about twice the moment of the S100du structure. This implies an additive effect in the contribution to the magnetic moment from the S monomers.

For the S100dd structure, no magnetism is found due to the strong S-S interaction because of the short S-S bond (2.05 Å) and the longer S-Mo bond (2.50 Å). This result is consistent within an effective medium theory⁴² picture, where a closer bond gives rise to a stronger interaction. The absence of magnetism is confirmed by the real space plots of the magnetization (Fig. 7) and the fact that the LDOS's for the spin-up and spin-down states are degenerate for both Mo and S atoms [Fig. 6(a)].

The magnetism of the S100du structure was discussed in Secs. III A and III B. Not only the edge Mo atoms but also the undimerized S atoms contribute to the magnetism [see Figs. 7 and 6(b)] due to the Mo-S hybridization. The Mo-S interaction is stronger if the S atoms are monomers owing to the shorter Mo-S distance (2.40 Å), as compared with the Mo to S dimer bond (2.49 Å).

For the S100uu structure, the Mo-S interaction is strong (the Mo-S distance is 2.42 Å) and the interaction between the S edge atoms is absent due to the large S-S distance (2.95 Å). The LDOS's [Fig. 6(c)] shows, apart from a splitting of the Mo states, a large splitting of the S states. The largest contribution to the magnetic moment for this structure is from the S atoms [$+0.13\mu_B$ compared with $-0.35\mu_B$ for the Mo atoms (see Table III)], in contrast to the other studied structures. With respect to the Mo or S atoms alone, this is a ferromagnetic structure. However, with respect to the total system, it is antiferromagnetic structure with a net magnetic moment, which can be compared with the magnetic configurations found for small Fe-S clusters.⁴³

In conclusion, our results of (i) the bond lengths, (ii) the strength of the magnetic moments, (iii) the LDOS's, and (iv) the real space localization of the magnetization confirm the validity of our hypothesis. A large magnetic moment is associated with the presence of strong Mo-S interactions, which

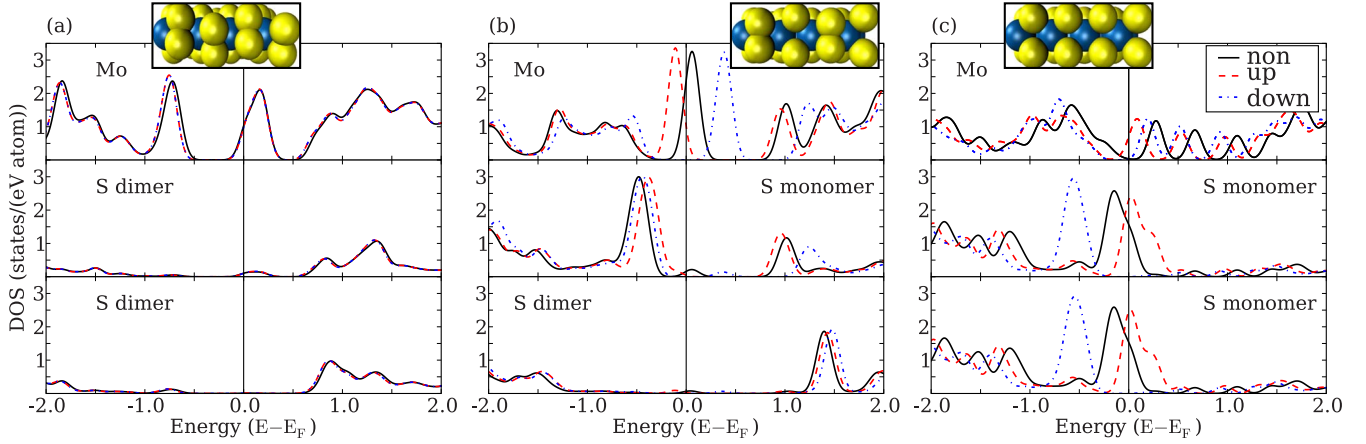


FIG. 6. (Color online) LDOS's for relevant edge Mo and S atoms of the: (a) S100dd, (b) the S100du, and (c) the S100uu structure.

results in magnetic edge S atoms. Hence, there is an intricate interplay between the S configuration at the edges and the appearance of magnetism.

IV. HYDROGEN ADSORPTION

For an MoS₂ nanoparticle to catalyze the HDS reaction, it must be able to both bind the sulfur-containing molecules and the hydrogen and to make it available for the hydrogenation steps. Therefore, under HDS conditions, H₂ is present and some edge terminations will contain adsorbed hydrogen. Hydrogen is activated by dissociative adsorption of H₂ on the MoS₂, previously studied in Refs. 44 and 45. After activation, hydrogen can react with the S of the adsorbed organic compound resulting in H₂S and a desulfurized organic molecule, which in turn can desorb from the surface. All these reactions take place at either the Mo or the S edge¹⁹ as opposed to the basal planes, which are inactive towards these reactions.

In this section we study the effect of the spin-spin interaction on the hydrogen adsorption on the MoS₂ edges. The presence of magnetic states that we have identified at the edges might cause a change in the H adsorption energies owing to the magnetic interaction between the edge atoms and the unpaired H electron.

The adsorption energy of H relative to H₂ is defined as

$$E_H = E[\text{MoS}_2 + x\text{H}] - E(\text{MoS}_2) - \frac{x}{2}E(\text{H}_2), \quad (2)$$

where the first term corresponds to the total energy of the MoS₂ stripe with x adsorbed H atoms and the second term is the total energy of the clean MoS₂ stripe.

The chosen initial structures for this study are structures that are relevant for HDS and are stable according to Ref. 6. We define the H coverage as the number of adsorbed H atoms per S edge atom. First non-spin-polarized then spin-polarized calculations are performed, in both steps allowing all the atoms to relax. The spin-polarized calculations were initialized with ferromagnetic symmetry with the initial magnetic moments of zero, $2\mu_B$, and $1\mu_B$ for the S, Mo, and H atoms, respectively. Hydrogen is only adsorbed on one edge

at a time while the other edge is fixed in the configuration with 100% S coverage.

In Table IV, the relaxed structures, the nomenclature, the energetics, and the magnetic moments of the considered structures are presented. We also specify at which edge termination(s) the magnetic states are localized.

The non-spin-polarized calculations show that the preferred hydrogenated structures are the Mo50H50 and the S100H50a structure for the Mo and the S edge, respectively. We also find that the chemical reactivity towards H adsorption is in general much higher on the S edge than on the Mo edge. The calculated H adsorption strengths are weaker than the ones found in Ref. 6, since the PW91 exchange functional is known to give stronger binding³² than the RPBE functional. However, we find that the relative stability order between the structures is the same for these two functionals.

All the hydrogenated Mo-edge structures have the same total magnetic moment, which is unchanged compared with the corresponding Mo-edge structure without H. This implies

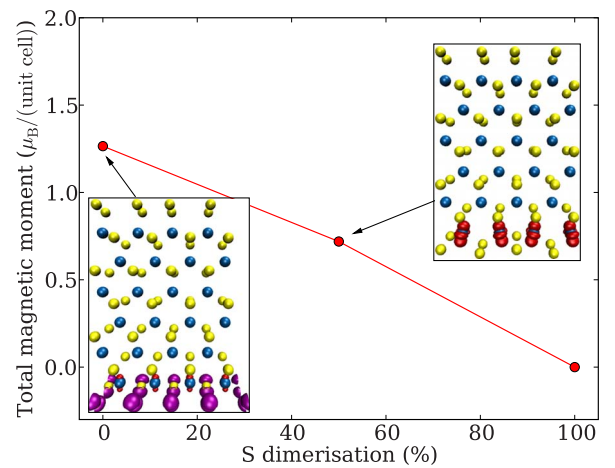
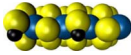
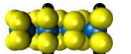
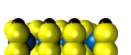
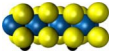
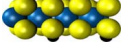
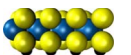
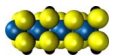
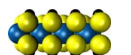


FIG. 7. (Color online) The total magnetic moment per edge Mo atom of the S100dd (100%), the S100du (50%) and the S100uu (0%) structure. Also illustrated is the localization of the magnetism (isosurface with $0.05/\text{\AA}^3$ is red and isosurface with $-0.05/\text{\AA}^3$ is purple). The nonmagnetic structure is not shown. For the S100uu structure, the edge S atoms are magnetic.

TABLE IV. (Color online) Relaxed atomic structures, nomenclature (Nom.) and H adsorption energies, E_H , for some relevant adsorption configurations on the Mo and S edge. $\Delta E_H^{\text{ferro}}$ is the energy difference per edge Mo atom between the ferromagnetic structure compared with the non-spin-polarized one. All energies are in eV. Also presented are the magnetic moments M , given in $\mu_B/(\text{Mo atom})$, and the edge [either S, Mo or none (-)] location of the magnetic states (Pos.). The Mo, S, and H atoms are represented as blue (gray), yellow (light), and black (black) balls, respectively.

Structure	Nom.	E_H	$\Delta E_H^{\text{ferro}}$	M_{tot}	Pos.
Mo edge					
	Mo50H50	-0.420	-0.031	0.394	S
	Mo100H50	0.206	-0.021	0.348	S
	Mo100H100	0.514	-0.021	0.353	S
S edge					
	S100H25	-0.315	0.000	0.006	S
	S100H50s	-0.469	-0.018	0.327	S
	S100H50a	-0.903	0.000	0.000	S
	S100H75	-0.859	0.000	0.035	S
	S100H100	-0.411	-0.091	0.752	S

that the magnetism is exclusively located on the S edge, also confirmed by visualizing the magnetization in real space and by investigating the LDOS's, and that the Mo-H and S-H interactions on the Mo edge have no magnetic contributions.

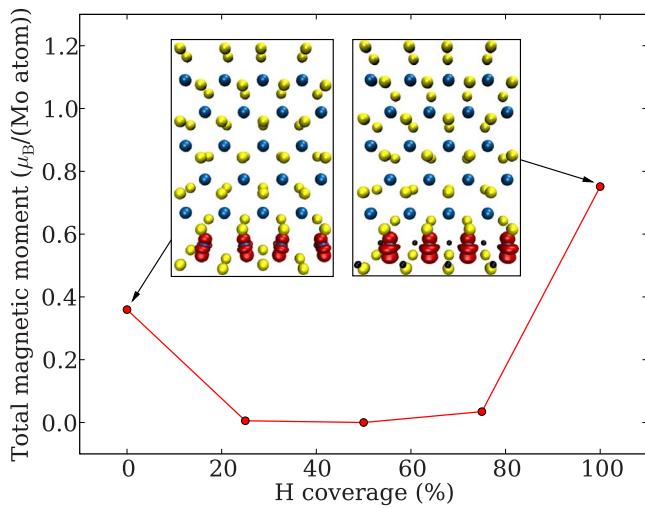


FIG. 8. (Color online) The total magnetic moment per Mo atom as a function of H coverage at the S edge (the Mo edge is H free). Also visualized are the atomic structures and the magnetization in real space of the magnetic stripes (the nonmagnetic ones are not shown). The color coding is the same as in Fig. 2 and the H atoms are represented as black balls.

For the S-edge structures, the S100H50s and the S100H100 structure have a significant magnetic moment (Fig. 8). The latter gains approximately 0.1 eV per Mo edge atom upon introduction of the spin-spin interaction. Figure 9 presents the LDOS for the S100H50 and the S100H100 structures, which should be compared with the results for the S100uu structure [see Table III and Fig. 6(c)]. Both the S100H50s and the S100H100 structures have a smaller magnetic moment than the S100uu structure. For the S100H50s structure, the magnetism originates from the splitting in the LDOS's of the Mo atoms and of the S atoms without adsorbed H, which is similar to the LDOS's for the S monomers for the S100uu structure. The S pairs with adsorbed H act towards the Mo atoms as if they were dimerized [see Fig. 6(c) and the discussion of the S dimerization on the magnetism in Sec. III C]. The LDOS's for the S100H100 structure shows that the large magnetic moments present at the S monomers [see Fig. 6(c)] are quenched because of the S-H bond. Instead a large magnetic moment is associated with the Mo edge atoms.

From thermodynamic considerations, the most stable stripe under HDS conditions is the one with 50% H-covered Mo edge and a H-covered S edge.^{6,19,29} Therefore, we expect MoS₂ nanoparticles under HDS conditions to be weakly magnetic.

V. SUMMARY AND DISCUSSION

We have investigated the magnetic properties of the Mo edge and the S edge of MoS₂ nanoparticles under STM and

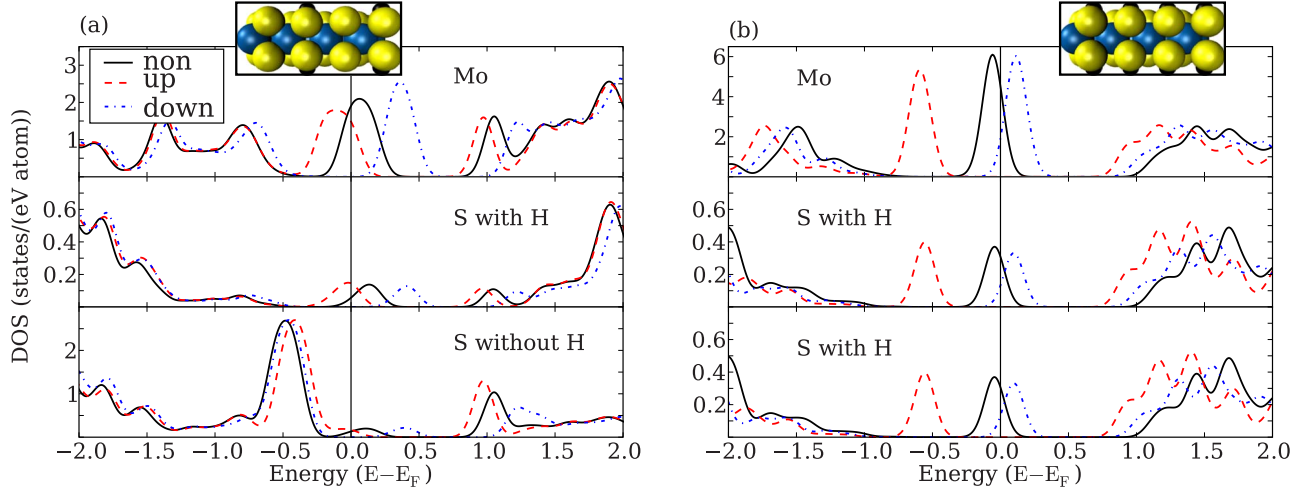


FIG. 9. (Color online) LDOS's for a Mo atom, an S atom from each S pair for (a) the S100H50s and (b) the S100H100 structure.

HDS conditions using a stripe model. Our model allows us to capture the magnetic contributions from the edges in an isolated way without corner effects. We consider different sulfur terminations of the edges, motivated by structures present under HDS conditions and under conditions of previous STM studies. Further, the influence of H on the magnetism was considered.

For the Mo edge, no magnetic structure is identified, which is present under STM or HDS conditions. Adsorption of H on the Mo edge does not lead to magnetic structures either. Hence, we do not expect the Mo edge to be magnetic under any relevant conditions.

For the S edge, magnetism is found for the S0 structure, not relevant under STM nor HDS conditions, the S100uu and the S100du structures, with only the latter one being relevant under HDS conditions. When it comes to H adsorption, the magnetism depends sensitively on the number of adsorbed H atoms. Magnetic structures relevant under HDS conditions are the S100H50s and the S100H100 structures.

We find that the magnetism originates from the splitting of the metallic edge states in the vicinity of the Fermi level. This is in agreement with spin-Peierls arguments.³⁹ We find that a large amount of states at the Fermi level for the nonmagnetic state results in a large splitting in the magnetic state and hence a large magnetic moment, known since Stoner.⁴⁰

Our findings show that the magnetic interaction will not significantly affect the phase diagram based on the non-spin-polarized calculations⁶ since the changes in sulfur formation energies and the hydrogen adsorption energies are small. This conclusion justifies the previous non-spin-polarized results for the MoS₂ systems.

In Ref. 27 calculations were performed on triangular nanoclusters terminated either by (with our nomenclature) only Mo0, Mo50, or Mo100 edges or only by S50 or S100uu edges. Magnetism was found for clusters with Mo0 and S100uu edges. This agrees well with our findings and our results have the same order of magnitude. However, we find that the Mo0 edge has a higher magnetic moment than the S100uu edge, in contrast to the findings in Ref. 27. This difference can be ascribed to the fact that the magnetization at the S edge is highly sensitive towards the configuration of

the S pairs, as shown in Sec. III C. Furthermore, the interaction between the cluster edges cannot be excluded due to the small cluster size considered in Ref. 27.

Let us consider the implication of our results on MoS₂ nanoparticles in the two situations (i) STM imaging conditions and (ii) working conditions for HDS catalysts. The shape of a nanoparticle depends on the relative free energies of the edges according to the Wulff construction.^{20,46} The free energies of MoS₂ particles for nonzero temperatures in the presence of H₂ and H₂S have been studied by employing the grand canonical formalism.^{6,20,47} For the considered cases it is known that the MoS₂ nanoparticles have (i) a triangular morphology, terminated by Mo100 edges,^{4,6} and (ii) hexagonal shape with different terminations depending on the chemical potentials of hydrogen, μ_H , and sulfur, μ_S .^{17,20,47} For low μ_H and μ_S , half of the edges are terminated by Mo50 edges, and the other half by S100du. When μ_H is high and μ_S small, half of the edges are Mo50H50 edges and the other half are either S100H100 or S100H50a depending on the hydrogen pressure. Our results imply that MoS₂ nanoparticles in case (i) should be nonmagnetic, and in case (ii) they should be magnetic.

For the weak magnetism to be measurable on a macroscopic level, there must be a large number of magnetic edge states. This is achievable if the amount of nanoparticles is large and if the particle size is not too big. The most suited particle size is the one that optimizes the ratio between the number of edge atoms to the number of bulk atoms and at the same time has a detectable amount of magnetic edge states.

The total magnetization (M_{tot}) of a particle is given by

$$M_{\text{tot}} = M \frac{N_{\text{edge}}}{N_{\text{tot}}} \frac{\mu_B}{m_{\text{particle}}} \quad [\text{in emu/g}], \quad (3)$$

where M is the strength of the local magnetic moment of a Mo edge atom that contributes to the magnetization, N_{edge} is the total amount of Mo edge atoms, N_{tot} is the total amount of Mo atoms in the particle, $\mu_B = 9.274 \cdot 10^{-21}$ emu and m_{particle} is the total mass of the particle in grams.

In the following, we estimate, based on our calculations, the magnetism of the MoS₂ nanoparticles employed in the experiment by Zhang *et al.*²⁷ and of hexagonal particles relevant under HDS conditions. Experimentally, triangle-shaped MoS₂ nanosheets have a magnetization of ~ 1 emu/g.²⁷ As Zhang *et al.* have not done any structural characterization of the particles, our estimate can only be qualitative.

Assume that we have a triangular particle terminated by only S100du edges, which is not present under HDS conditions. A triangular particle has $N_{\text{edge}}=3(n-1)$ with n being the number of Mo edge atoms per triangle edge and $N_{\text{tot}}=(n^2+n)/2$. For a particle of edge size 100 nm (an estimate based on SEM images in Ref. 27), we obtain a magnetization of 0.24 emu/g. If, on the other hand, the particle is terminated by only S100uu edges, the magnetization is 0.42 emu/g, again reflecting the delicate dependence of the magnetization on the S configuration at the S edge and the difference in magnetization between a finite sized particle and an infinite stripe. Even though this particle is not relevant under HDS conditions, it gives a rough estimate of the upper boundary of the magnetization, since it is the limit of a hexagonal particle with vanishingly small contribution from the Mo edges. The lower limit is given by a triangular terminated by Mo100 edges, which is not magnetic.

Consider a regular hexagonal particle inscribed in the circle with the same radius as the radius of the circle circumscribing a triangle with the edge side of 100 nm. The hexagon-edge size is 58 nm and it consists of $n=181$ Mo edge atoms. The particle has three edges terminated by a Mo edge and three edges terminated by a S edge. Only the S edges contribute to the magnetization and therefore $N_{\text{edge}}=6(n-1)/2$. The total amount of Mo atoms is given by $N_{\text{tot}}=3n(n-1)+1$. This implies that the hexagonal particle partly terminated by (a) S100du edges has a magnetization of

0.07 emu/g, (b) S100H50a edges are not magnetic, and (c) S100H100 edges has magnetization of 0.15 emu/g. The obtained magnetization values are in the interval estimated above for the triangular particles terminated either by only Mo edges or S edges.

We find that the magnetic properties of a MoS₂ nanoparticle depend on its edges and hence its shape, which in turn depends on the working conditions. At certain temperatures the MoS₂ nanoparticle should undergo phase transitions from magnetic to nonmagnetic. In Ref. 48 it was found that the magnetic moment changes upon changes in particle morphology, however, we cannot make any quantitative comparisons due to the scarce information of the structural characterization. For the triangular particles, our estimates have the same order of magnitude as the results in Ref. 27.

Our results have interesting implications for the monitoring of magnetic properties in, e.g., electron paramagnetic resonance (EPR) measurements and how well these measurements reflect the catalytic properties. We find that large changes in magnetic moments are accompanied by very small changes in energy (in the order of or smaller than thermal energies), e.g., for structures terminated by S100du, S100H50a, and S100H100 edges. However, EPR measurements are often used to monitor catalytic cycles.⁴⁹ In view of our results, a direct mapping of the changes in magnetic and catalytic properties is not possible in the case of MoS₂ systems, as large changes in magnetic moments are not indicative of correspondingly large energetic changes, which could also be the case for other systems.

ACKNOWLEDGMENTS

The calculations were performed at NSC via the Swedish National Infrastructure for Computing (SNIC) and the Danish Center for Scientific Computing.

*alevoj@chalmers.se

¹A. K. Geim and K. S. Novoselov, Nat. Mater. **6**, 183 (2007).

²M. Fujita, K. Wakabayashi, K. Nakada, and K. Kusakabe, J. Phys. Soc. Jpn. **65**, 1920 (1996).

³P. L. Giunta and S. P. Kelty, J. Chem. Phys. **114**, 1807 (2001).

⁴M. V. Bollinger, J. V. Lauritsen, K. W. Jacobsen, J. K. Nørskov, S. Helveg, and F. Besenbacher, Phys. Rev. Lett. **87**, 196803 (2001).

⁵S. Helveg, J. V. Lauritsen, E. Lægsgaard, I. Stensgaard, J. K. Nørskov, B. S. Clausen, H. Topsøe, and F. Besenbacher, Phys. Rev. Lett. **84**, 951 (2000).

⁶M. V. Bollinger, K. W. Jacobsen, and J. K. Nørskov, Phys. Rev. B **67**, 085410 (2003).

⁷J. V. Lauritsen, M. Nyberg, R. T. Vang, M. V. Bollinger, B. S. Clausen, H. Topsøe, K. W. Jacobsen, E. Lægsgaard, J. K. Nørskov, and F. Besenbacher, Nanotechnology **14**, 385 (2003).

⁸K. Nakada, M. Fujita, G. Dresselhaus, and M. S. Dresselhaus, Phys. Rev. B **54**, 17954 (1996).

⁹K. Wakabayashi, M. Fujita, H. Ajiki, and M. Sigrist, Phys. Rev. B **59**, 8271 (1999).

¹⁰Y.-W. Son, M. L. Cohen, and S. G. Louie, Phys. Rev. Lett. **97**, 216803 (2006).

¹¹V. Barone, O. Hod, and G. E. Scuseria, Nano Lett. **6**, 2748 (2006).

¹²H. H. Lin, T. Hikiyama, H. T. Jeng, B. L. Huang, C.-Y. Mou, and X. Hu, Phys. Rev. B **79**, 035405 (2009).

¹³L. Rapoport, Y. Bilik, Y. Feldman, M. Homoyonfer, S. R. Cohen, and R. Tenne, Nature **387**, 791 (1997).

¹⁴M. Chhowalla and G. A. J. Amaratunga, Nature (London) **407**, 164 (2000).

¹⁵H. Topsøe, B. S. Calusen, and F. E. Masooth, *Hydrotreating Catalysis* (Springer, Berlin, 1996).

¹⁶J. V. Lauritsen, S. Helveg, E. Lægsgaard, I. Stensgaard, B. S. Clausen, H. Topsøe, and F. Besenbacher, J. Catal. **197**, 1 (2001).

¹⁷J. V. Lauritsen, M. V. Bollinger, E. Lægsgaard, K. W. Jacobsen, J. K. Nørskov, B. S. Clausen, H. Topsøe, and F. Besenbacher, J. Catal. **221**, 510 (2004).

¹⁸J. V. Lauritsen, J. Kibsgaard, G. Olesen, P. G. Moses, B. Hinneemann, S. Helveg, J. K. N. B. S. Clausen, H. Topsøe, E. Lægsgaard, and F. Besenbacher, J. Catal. **249**, 220 (2007).

- ¹⁹P. G. Moses, B. Hinnemann, H. Topsøe, and J. K. Nørskov, *J. Catal.* **248**, 188 (2007).
- ²⁰P. Raybaud, J. Hafner, G. Kresse, S. Kasztelan, and H. Toulhoat, *J. Catal.* **189**, 129 (2000).
- ²¹M. Sun, A. E. Nelson, and J. Adjaye, *J. Catal.* **226**, 32 (2004).
- ²²T. Todorova, R. Prins, and T. Weber, *J. Catal.* **246**, 109 (2007).
- ²³M. Remškar, A. Mrzel, Z. Skraba, A. Jesih, M. Ceh, J. Demšar, P. Stadelmann, F. Lévy, and D. Mihailović, *Science* **99**, 016105 (2001).
- ²⁴Z. Jagličić *et al.*, *Polyhedron* **22**, 2293 (2003).
- ²⁵M. Verstraete and J.-C. Charlier, *Phys. Rev. B* **68**, 045423 (2003).
- ²⁶P. Murugan, V. Kumar, Y. Kawazoe, and N. Ota, *Phys. Rev. A* **71**, 063203 (2005).
- ²⁷J. Zhang, J. M. Soon, K. P. Loh, J. Yin, J. Ding, M. B. Sullivan, and P. Wu, *Nano Lett.* **7**, 2370 (2007).
- ²⁸B. Hinnemann, P. G. Moses, J. Bonde, K. P. Jørgensen, J. H. Nielsen, S. Horch, I. Chorkendorff, and J. K. Nørskov, *J. Am. Chem. Soc.* **127**, 5308 (2005).
- ²⁹B. Hinnemann, J. K. Nørskov, and H. Topsøe, *J. Phys. Chem. B* **109**, 2245 (2005).
- ³⁰S. R. Bahn and K. W. Jacobsen, *Comput. Sci. Eng.* **4**, 56 (2002).
- ³¹<http://wiki.fysik.dtu.dk/dacapo>.
- ³²B. Hammer, L. B. Hansen, and J. K. Nørskov, *Phys. Rev. B* **59**, 7413 (1999).
- ³³L. Bengtsson, *Phys. Rev. B* **59**, 12301 (1999).
- ³⁴T. Böker, R. Severin, A. Müller, C. Janowitz, R. Manzke, D. Voß, P. Krüger, A. Mazur, and J. Pollmann, *Phys. Rev. B* **64**, 235305 (2001).
- ³⁵P. G. Moses, J. J. Mortensen, B. I. Lundqvist, and J. K. Nørskov, *J. Chem. Phys.* **130**, 104709 (2009).
- ³⁶R. F. W. Bader, *Chem. Rev.* **91**, 893 (1991).
- ³⁷G. Henkelman, A. Arnaldsson, and H. Jonsson, *Comput. Mater. Sci.* **36**, 354 (2006).
- ³⁸R. O. Jones and O. Gunnarsson, *Rev. Mod. Phys.* **61**, 689 (1989).
- ³⁹R. Peierls, *Quantum Theory of Solids* (Oxford University Press, London, 1955).
- ⁴⁰E. C. Stoner, *Proc. R. Soc. Lond. A Math. Phys. Sci.* **165**, 372 (1938).
- ⁴¹O. Gunnarsson, *J. Phys. F: Met. Phys.* **6**, 587 (1976).
- ⁴²J. K. Nørskov and N. D. Lang, *Phys. Rev. B* **21**, 2131 (1980).
- ⁴³B. Hinnemann and J. K. Nørskov, *Phys. Chem. Chem. Phys.* **6**, 843 (2004).
- ⁴⁴J. F. Paul and E. Payen, *J. Phys. Chem.* **107**, 4057 (2003).
- ⁴⁵M. Sun, A. E. Nelson, and J. Adjaye, *Catal. Today* **105**, 36 (2005).
- ⁴⁶G. Wulff, *Z. Kristallogr.* **34**, 449 (1901).
- ⁴⁷H. Schweiger, P. Raybaud, G. Kresse, and H. Toulhoat, *J. Catal.* **207**, 76 (2002).
- ⁴⁸S. K. Srivastava and B. N. Avasthi, *J. Mater. Sci.* **28**, 5032 (1993).
- ⁴⁹P. Dos Santos, R. Y. Igarashi, H.-I. Lee, B. M. Hoffman, L. C. Seefeldt, and D. R. Dean, *Acc. Chem. Res.* **38**, 208 (2005).